International Journal of Mass Spectrometry 277 (2008) 229–235

Contents lists available at ScienceDirect

International Journal of Mass Spectrometry

journal homepage: www.elsevier.com/locate/ijms

Collisions of slow hydrocarbon ions $CD_4^{\bullet+}$, CD_5^+, $C_2D_4^{\bullet+}$, and $C_2H_5^+$ with room temperature and heated tungsten surfaces

Andriy Pysanenko[a], Jan Žabka[a], Tilmann D. Märk[b], Zdenek Herman[a,b,*]

[a] V. Čermák Laboratory, J. Heyrovský Institute of Physical Chemistry, v.v.i., Academy of Sciences of the Czech Republic, Dolejškova 3, 182 23 Prague 8, Czech Republic
[b] Institut für Ionenphysik und Angewandte Physik, Leopold-Franzens Universität Innsbruck, Techniker Str. 25, 6020 Innsbruck, Austria

ARTICLE INFO

Article history:
Received 18 March 2008
Received in revised form 6 May 2008
Accepted 20 May 2008
Available online 27 May 2008

Keywords:
Surface-induced process
Hydrocarbon ion
Tungsten surface
Ion survival probability
Surface scattering

ABSTRACT

The interaction of selected hydrocarbon ions with tungsten surfaces, at room temperature and heated to 600 °C, was investigated at incident energies of 15–45 eV and at incident angles of 60° and 45° to the surface normal. Results were compared with earlier published studies on carbon (highly oriented pyrolytic graphite, HOPG) surfaces. The ion survival probability for both room temperature and heated W surfaces was in general a factor of 2–15 smaller than on carbon (HOPG) surfaces and tended to be smaller for radical cations ($CD_4^{\bullet+}$ and $C_2D_4^{\bullet+}$) than for closed-shell ions (CD_5^+ and $C_2H_5^+$). Mass spectra, translational energy distributions and angular distributions of product ions from collisions with W surfaces were very similar to distributions estimated earlier for carbon (HOPG) surfaces. Mass spectra of radical cations on room temperature surfaces indicated fragmentation of projectile ions and reactions (of H-atom transfer and carbon-chain build-up) with hydrocarbons on the surface. Closed-shell ions showed only fragmentation processes. On heated surfaces, only fragmentations of the incident projectile ions were observed. The similarity of results on heated tungsten and HOPG surfaces may be due to substantial coverage of W surfaces with tungsten carbides originating from cracked surface hydrocarbons.

1. Introduction

The interaction of hyperthermal ions with surfaces is of interest for both fundamental and practical reasons. Investigation of selected physical and chemical processes induced by impact of ions of energies below 100 eV on surfaces has found, over the last two decades, many applications [1–6] ranging from surface diagnostics and surface modifications to characterization of projectile ions. Surface-induced activation and fragmentation of projectile ions has been used as one of the methods for characterizing structural properties of polyatomic ions from relatively simple ions [7–9] to large biomolecules [10–18].

Ion-surface collisions can be an important source of information relevant to plasma-wall interactions in fusion systems [5]; this article is motivated in part by the requirement to understand this issue. Consideration of tungsten and beryllium, in addition to carbon, as a possible first wall material in the ITER tokamak has been recently emphasized. The need to understand issues such as wall erosion, transport and re-deposition of eroded material, transient heat loads, and plasma-edge physics related to material erosion have been stressed [19]. In addition, measurements will be of general interest in understanding surface interactions of slow polyatomic ions.

In our earlier papers, we described the use of the ion-surface scattering method in obtaining information on interactions of hydrocarbon and other projectile ions with carbon surfaces [20–24]. Data on projectile ion survival probability in collisions with room temperature and heated (600 °C) carbon surfaces, on fragmentation processes and chemical reactions at surfaces, and on energy partitioning in surface collisions were obtained. The projectiles were simple hydrocarbon cations C1 [20,24], C2 [22], cations and dications $C_7H_n^{+/2+}$ (n = 6, 7 and 8) [23], and model ethanol ions [21]. One of the important findings of these studies was a large difference between survival probabilities in surface collisions of different ions. Ions with recombination energies below 10 eV (usually closed-shell ions) exhibited survival probabilities of up to tens of percent [20,22,23], whilst ions of recombination energies about 10–11 eV (usually radical cations) showed survival probabilities 50–100 times smaller [20,22] than for closed-shell ions.

In this paper we investigate collisions of slow (15–50 eV) hydrocarbon ions with room temperature and heated tungsten surfaces. The projectile ions were reactive radical cations $CD_4^{\bullet+}$ and $C_2D_4^{\bullet+}$ and closed-shell chemically non-reactive cations CD_5^+ and $C_2H_5^+$, taken as representatives of C1 and C2 hydrocarbon ions, respec-

* Corresponding author at: V. Čermák Laboratory, J. Heyrovský Institute of Physical Chemistry, v.v.i., Academy of Sciences, Dolejškova 3, 182 23 Prague 8, Czech Republic. Tel.: +420 2 66 053 514; fax: +420 2 86 582 307.
E-mail address: zdenek.herman@jh-inst.cas.cz (Z. Herman).

1387-3806/$ – see front matter © 2008 Elsevier B.V. All rights reserved.
doi:10.1016/j.ijms.2008.05.024

tively. The surface was a tungsten sample at room temperature or heated to 600 °C. Results of ion-surface scattering experiments in which mass spectra, translational energy and angular distributions of product ions are measured with respect to incident angle and energy of selected projectile ions are described. From the measured data, we determine ion survival probabilities and characterize surface fragmentation processes and surface chemical reactions. Translational energy distributions of the product ions were used to determine the inelasticity of the collisions and contributed to estimation of energy partitioning in the surface collisions. The objective of the paper was to compare the results on ion survival probability, fragmentation, chemical reactions and energy transfer at room temperature and heated tungsten surfaces with earlier measurements for carbon surfaces.

2. Experimental

2.1. Apparatus

The experiments were carried out with the Prague beam scattering apparatus EVA II modified for ion-surface collision studies. The application of the apparatus to the described studies was described earlier [20–26]. Briefly, projectile ions were formed by electron impact ionization (120 eV) of methane or ethane (or their deuterated variants). The ions were extracted, accelerated to about 150–300 eV, mass analyzed by a 90° permanent magnet, and decelerated to the required energy in a multi-element deceleration lens. The resulting beam had an energy spread of 0.2 eV, full-width-at-half-maximum (FWHM), angular spread of 1.5° (FWHM), and geometrical dimensions of 0.4 mm × 1.0 mm. The beam was directed towards a tungsten target surface under a pre-adjusted incident angle Φ_N (here 60° or 45° with respect to the surface normal), set by laser beam reflection with a precision of about 1°. Ions scattered from the surface passed through a detection slit into a stopping potential energy analyzer. After energy analysis the ions were focused and accelerated into a detection mass spectrometer (a magnetic sector instrument), and detected by counting the ions at the output of a Galileo channel multiplier. The primary beam exit slit, the target, and the detection slit were kept at the same potential and carefully shielded by μ-metal sheets. The primary beam-target section could be rotated about the scattering center with respect to the detection slit to obtain angular distributions. The incident (Φ_N) and scattering (Θ'_N) angles were measured with respect to the surface normal.

The apparatus was evacuated by 1380 l/s (scattering chamber) and 56 l/s (detector-mass spectrometer region) turbomolecular pumps backed by rotary vacuum pumps. The background pressure in the apparatus was about 5×10^{-7} Torr, and during the experiments the pressure was about 5×10^{-6} Torr due to the leakage of the source gas into the scattering chamber. Despite the molecular sieve trap, the use of rotary vacuum pumps led to a small backstreaming of rotary oil vapor into the scattering chamber. As a result, the surface of the tungsten sample was covered at room temperature with a layer of hydrocarbons. This layer could be removed by heating the surface to 600 °C or higher (as tested by the absence of H-atom transfer reactions between radical cations and surface material). Cooling back to room temperature led to a renewal of the hydrocarbon layer in less than 1 h.

2.2. Tungsten surface

The tungsten surface target was a 99.9% tungsten sheet, 0.05 mm thick (Aldridge Chemical Comp.). Before placing it into vacuum, the surface was either mechanically or electrochemically polished. Electrolytic polishing followed the standard procedure of dipping the sample, as anode for 30 s into a 20% solution of NaOH in water. The sample was mounted into a stainless steel holder located 10 mm in front of the exit slit of the projectile ion deceleration system. The tungsten target surface in the experiments was kept either at room temperature or at an elevated temperature of about 600 °C. For this purpose, the sample was resistively heated and its temperature measured by a thermocouple and/or by a pyrometer. The absence of the H-atom transfer reaction with surface hydrocarbons indicated that heating the surface to 600 °C or higher decreased the concentration of hydrocarbons on the surface more that 100 times [20,22]. The temperature of 600 °C was thus regarded as sufficiently high effectively to remove the hydrocarbon layer covering the surface at room temperature. At sample temperatures above 500 °C, emission of K^+ ions from the sample, increasing with temperature, was observed.

When the tungsten sample was first placed into vacuum and kept at room temperature, the mass spectrum of scattered ions showed, besides inelastically scattered product ions, a contribution from incident projectile ions having full incident energy and narrow energy distribution. Because their energy was higher than the energy of the scattered product ions, their apparent mass depended on the incident energy and appeared in the mass spectra at a slightly higher apparent mass increasing with increasing incident energy. This component, with a new unheated W sample, was up to 5% of the incident ion current. Heating the sample in vacuum and cooling it to room temperature decreased this projectile ion component to 0.05% of the incident ion current. We interpreted this component as a fraction of the incident beam which was deflected in front of the surface by surface charges thereby not colliding with the surface at all (see also Ref. [25]).

Subsequent ex situ XPS analysis of the tungsten surfaces was performed. XPS spectra of mechanically or electrochemically cleaned W sample, placed into vacuum and kept at room temperature (unheated) in the apparatus, showed the presence of tungsten oxides, small amounts of tungsten carbide, and C–H groups on the surface (evidently adsorbed hydrocarbons). Heating or repeated heating of the W sample to 600 °C in vacuum led to a substantial decrease of the W oxides and to a sharp increase of tungsten carbide peaks (about 2.5 times with respect to unheated sample) in the XPS spectra. Therefore, it appears that heating the sample led to degradation of the surface hydrocarbons and formation of a substantial amount of tungsten carbides on the surface. In our opinion, these observations indicate the following: for a fresh sample, the presence of micro-islands of insulating tungsten oxides caused deflection of a fraction of projectile ions with full energy in front of the surface (see also Ref. [24]); heating the sample decreased the amount of oxides on the surface and strongly increased the amount of (apparently non-insulating) tungsten carbides. The projectile beam incident on the heated W surface thus presumably collided not only with tungsten atoms, but also with surface carbon atoms.

3. Results and discussion

3.1. Ion survival probability

The ion survival probability, S_a, is the percentage of ions surviving the surface collision. It is defined as a ratio of the sum of intensities of all ions scattered from the target, $\sum I_{PT}$, to the intensity of the projectile reactant ions incident on the target, I_{RT}, expressed as a percentage: $S_a = 100 \times \sum I_{PT}/I_{RT}$ (here $I_{RT} = I_{RTM} + \sum I_{PT}$, where I_{RTM} is the current of projectile ions actually measured on the target). The quantities measured directly in

the experiments were I_{RTM}, and the ion currents of product ions reaching the detector, $\sum I_{PD}$ (calculated from the count rates at the output of the multiplier). The equivalent current of all product ions scattered from the target surface, $\sum I_{PT}$, was estimated from the measured $\sum I_{PD}$, the discrimination of the apparatus (D_A), and the angular discrimination of the scattering differential measurements $D(\omega)_P/D(\omega)_R$, where $D(\omega)_P$ is the angular distribution of the product ions and $D(\omega)_R$ that of the reactant ions. The procedure used in the estimation of S_a was described in detail in our previous papers [20,22,24]. It leads to an expression for the absolute survival probability $S_a = 100FS_{eff}$, where the effective survival probability, $S_{eff} = \sum I_{PD}/I_{RT}$, consists of the measurable quantities whereas the factor F summarizes all discrimination effects.

Apparatus discrimination effects were estimated as the ratio of the ion current entering the detection slit, I_{RS}, to the ion current reaching the detector, I_{RD}, $D_A = I_{RS}/I_{RD}$. In the present experiments $D_A = 0.62 \times 10^2$. The angular discrimination factor, $D(\omega)_P/D(\omega)_R$, was approximated by the squared ratio of the mean width (FWHM) of the product ion angular distribution, Ω_P(FWHM), to the acceptance angle of the detection slit, Ω_{DS}, $D(\omega)_P = \Omega_P^2/\Omega_{DS}^2$, and by the analogous value for the reactant ion angular distribution (Ω_R), $D(\omega)_R = \Omega_R^2/\Omega_{DS}^2$. This gives $D(\omega)_P/D(\omega)_R = \Omega_P^2/\Omega_R^2$. The factor F in the present measurements was then $F = D_A[D(\omega)_P/D(\omega)_R]$. For Ω_R(FWHM) = 1.5°, $F = 27.6\Omega_P^2$, where Ω_P^2 was the square of the product ion angular distribution (FWHM) as determined from the angular distribution measurements.

The values of S_a for collisions of the above-mentioned projectile ions with both the room temperature and heated tungsten surface are given in Table 1. The uncertainties quoted are standard deviations derived from repeated measurements and/or estimated from the noise of signals in mass spectra measurements. All data are for the incident angle of 60°. In addition, data for $C_2D_4^+$ contain survival probabilities for the incident angle of 45° (Table 1, lines W(45°)). For comparison, we included into this table our earlier data for S_a of the hydrocarbon ions (at incident angle 60°) colliding with carbon (highly oriented pyrolytic graphite, HOPG) surfaces [20,22].

In general, the ion survival probability on tungsten was found to be smaller than on carbon (HOPG) and seldom exceeded 1%.

Table 1
Survival probabilities S_a (%) of hydrocarbon ions on room temperature and heated (600 °C) surfaces of tungsten and carbon (HOPG) [20,22]

	Surface	Incident energy (eV)		
		15.4	30.9	45.4
Room temperature				
$CD_4^{\bullet+}$	W	0.03 ± 0.01	0.033 ± 0.01	0.12 ± 0.04
	HOPG	0.37 ± 0.1	0.34 ± 0.2	0.27 ± 0.2
CD_5^+	W	4.7 ± 0.7	0.8 ± 0.1	1.2 ± 0.1
	HOPG	12.5 ± 5	12 ± 5	(18 ± 7)
$C_2D_4^{\bullet+}$	W	0.17 ± 0.04	0.17 ± 0.04	0.19 ± 0.04
	W(45°)	0.05 ± 0.02	0.10 ± 0.02	0.04 ± 0.02
	HOPG	1.0 ± 0.5	1.0 ± 0.4	0.9 ± 0.2
$C_2H_5^+$	W	2.7 ± 0.7	1.6 ± 0.5	0.85 ± 0.3
	HOPG	1.1 ± 0.03	1.0 ± 0.1	0.3 ± 0.03
Heated				
$CD_4^{\bullet+}$	W	0.03 ± 0.01	0.02 ± 0.007	0.02 ± 0.007
	HOPG	0.5	0.23	
CD_5^+	W	1.1 ± 0.3	0.5 ± 0.04	0.5 ± 0.04
	HOPG			(23)
$C_2D_4^{\bullet+}$	W	0.16 ± 0.05	0.1 ± 0.03	0.14 ± 0.04
	W(45°)	0.01 ± 0.01	0.07 ± 0.03	0.04 ± 0.02
	HOPG	0.35	0.4 ± 0.05	
$C_2H_5^+$	W	0.58 ± 0.1	0.32 ± 0.1	0.24 ± 0.1

Incident angle 60° (for $C_2D_4^+$–W(45°) also 45°).

For room temperature (hydrocarbon-covered) surfaces the ratio S_a(HOPG)/S_a(W) varied between 2 and 15, with the exception of $C_2H_5^+$ collisions, where S_a values for both types of surfaces was equal. For heated surfaces (with hydrocarbon layer practically removed) the survival probability on tungsten surfaces was smaller, too, but the ratio varied from 2 to 4 ($C_2D_4^{\bullet+}$) to more than 10 ($CD_4^{\bullet+}$). Otherwise, the survival probability on tungsten shows the same tendency as on carbon (HOPG): S_a was very small for the radical cation $CD_4^{\bullet+}$ (0.02–0.12%), somewhat (2–3 times) larger for the radical cation $C_2D_4^{\bullet+}$, and considerably larger (10–100 times, about

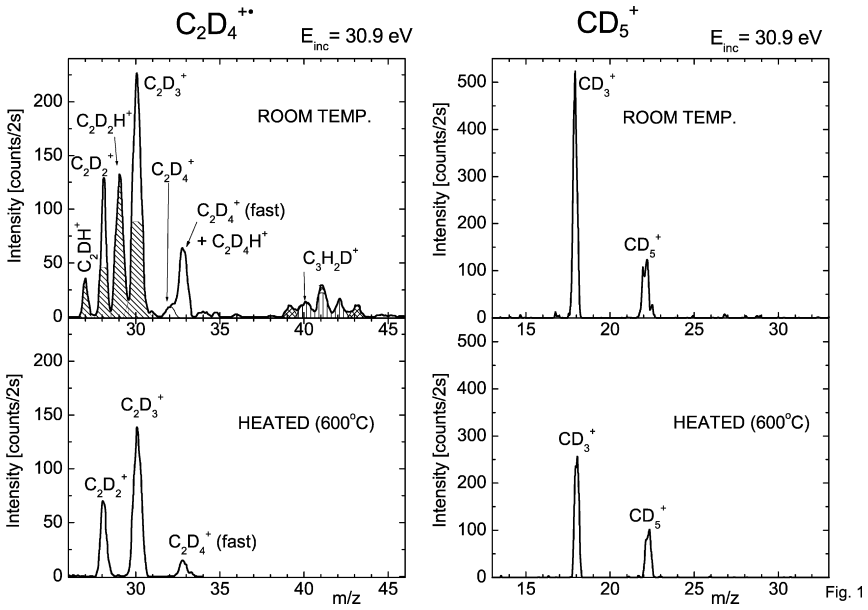

Fig. 1

Fig. 1. Mass spectra of product ions from surface interaction of $C_2D_4^{\bullet+}$ (left) and CD_5^+ (right) with room temperature and heated tungsten surfaces. Incident energy 30.9 eV, incident angle 60°; hatched: estimated contribution from H-atom transfer reaction with surface hydrocarbons; vertically hatched: estimated contribution of reaction of carbon-chain build-up; crossed hatched: background from sputtering of surface material.

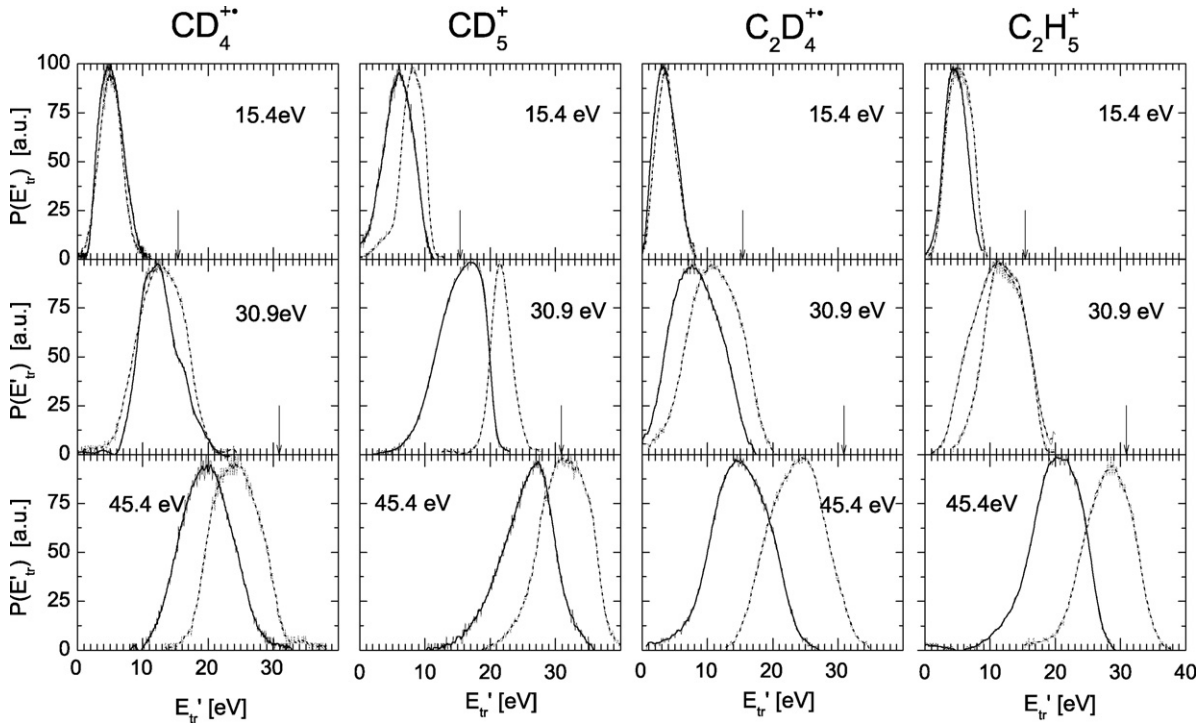

Fig. 2. Translational energy distributions of product ions from collisions of $CD_4^{\bullet+}$, CD_5^+, $C_2D_4^{\bullet+}$, and $C_2H_5^+$ with room temperature (solid line) and heated (dashed) tungsten surfaces at incident energies of 15.4 eV, 30.9 eV, and 45.4 eV. Incident angle 60°. Vertical arrows indicate the incident energy.

1% or higher) for the closed-shell cations CD_5^+ and $C_2H_5^+$. When decreasing the incident angle from 60° to 45°, S_a(W) decreased in most cases by a factor of 2–5, in agreement with earlier data for polyatomic ions on hydrocarbon-covered stainless steel [25], where the decrease was approximately a factor of 5 over the same range of incident angles.

3.2. Mass spectra of product ions

Product ion mass spectra from collisions of $CD_4^{\bullet+}$, CD_5^+, $C_2D_4^{\bullet+}$, and $C_2H_5^+$ projectile ions with room temperature and heated surfaces were measured at incident energies of 15.4 eV, 30.9 eV, and 45.4 eV. For simplicity, we include the inelastically scattered undis-

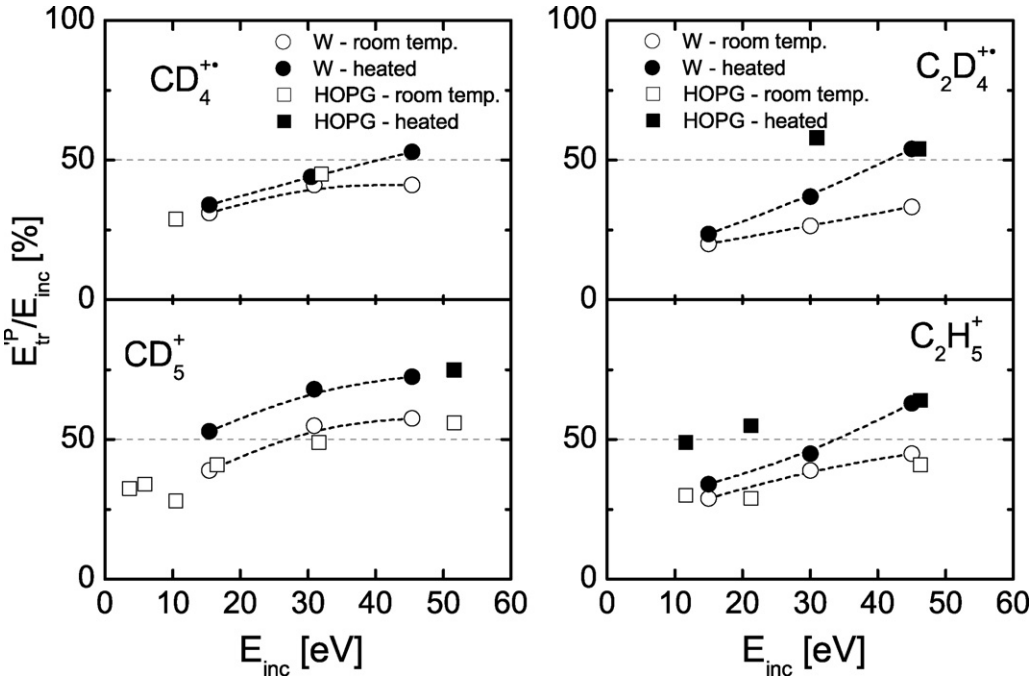

Fig. 3. The ratio of peak translational energy of product ions to incident energy, E'^{P}_{tr}/E_{inc} (fraction of incident energy in product translation in percent) as a function of the incident energy for collisions of $CD_4^{\bullet+}$, CD_5^+, $C_2D_4^{\bullet+}$, and $C_2H_5^+$ with tungsten (points) and carbon (HOPG) (squares) surfaces. Open symbols: room temperature surfaces; full symbols: heated (600 °C) surfaces.

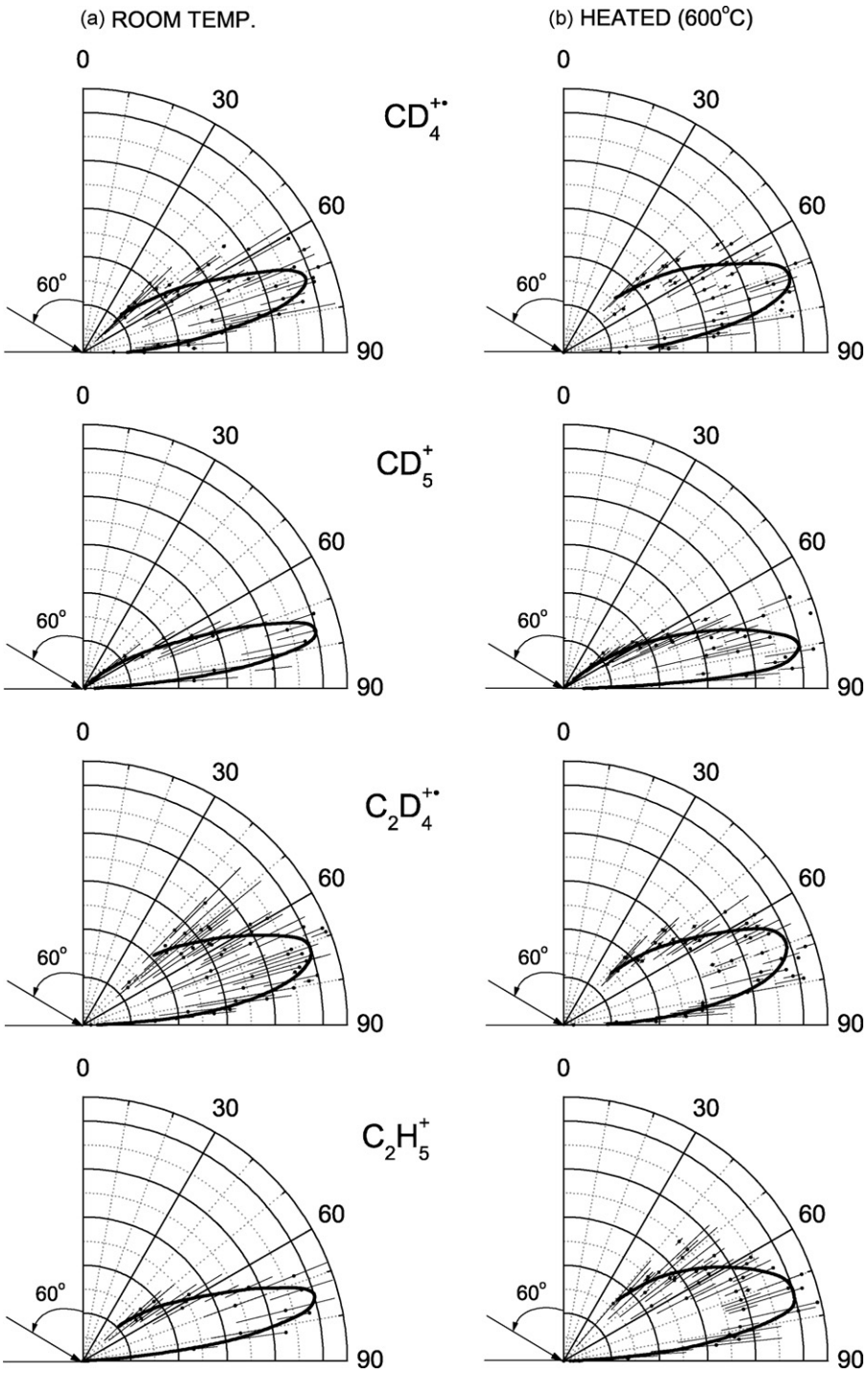

Fig. 4. Examples of polar plots of angular distributions of product ions from collisions of $CD_4^{\bullet+}$, CD_5^+, $C_2D_4^{\bullet+}$, and $C_2H_5^+$ with room temperature (a) and heated (b) tungsten surfaces. Incident energy 30.9 eV; incident angle 60°.

sociated incident ion with the product ions. The mass spectra were very similar to those of collisions between these ions with room temperature and heated surfaces of carbon (HOPG) [20,22], both in the extent of fragmentation of the incident ion, in chemical reactions with the surface material on the room temperature surface, and in the ratio of the contributions of direct fragmentation to surface chemical reactions. As for room temperature carbon surfaces, the main chemical reactions were H-atom transfer and $C_mX_n^+$ ($m = 2$ and 3; X = D and H) ion formation in reactions of the radical cations $CD_4^{\bullet+}$ and $C_2D_4^{\bullet+}$ with terminal CH_3– groups of the surface hydrocarbons [20,22]. Collisions of the closed-shell projectile ions CD_5^+ and $C_2H_5^+$ with W surface at room temperature showed only fragmentation of the projectile ion. On heated surfaces only fragmentation processes were observed for all studied ions.

Examples of mass spectra are given in Fig. 1 for collisions of $C_2D_4^{\bullet+}$ and $CD_5^{\bullet+}$ with incident energy of 30.9 eV on room temperature and heated (600 °C) tungsten surfaces. On the room temperature surface, the radical cation $C_2D_4^{\bullet+}$ shows simple fragmentation to $C_2D_3^+$ and $C_2D_2^{\bullet+}$, H-atom transfer reactions (forming $C_2D_4H^+$ and its dissociation products $C_2D_3^+$ and $C_2D_2H^+$, $C_2D_4^{\bullet+}$

and $C_2DH^{\bullet+}$—hatched in Fig. 1), and carbon-chain build-up reactions with surface hydrocarbons leading eventually to $C_3X_3^+$ (X = H and D) (vertically hatched in Fig. 1, see also Ref. [22]). On the heated W surface, the chemical reactions were no longer observable; only fragmentation of the incident projectiles was observed. This was attributed to the strong decrease in hydrocarbon coverage on the surface [20,22]. With the closed-shell CD_5^+ projectile, only partial fragmentation to CD_3^+ was observed.

3.3. Translational energy distributions of product ions

Translational energy distributions of product ions, $P(E'_{tr})$, from collisions with room temperature (solid line) and heated (dashed) tungsten surfaces are shown in Fig. 2. The incident angle of the projectile ions was 60°. Within experimental error, velocity distributions of scattered undissociated projectile ions and major fragment ions peaked at the same velocity were very similar. This indicated, in agreement with our earlier findings [20–26], that surface-induced projectile ion fragmentation occurred predominantly after interaction with the surface in a unimolecular manner. The $P(E'_{tr})$ data in Fig. 2 refer to inelastically scattered undissociated product ions whenever possible; at higher collision energies, when the signal of undissociated product ion was not measurable, the data were recalculated from translational energy distributions of the fragment ions (CD_3^+, $C_2D_3^+$ and $C_2H_3^+$) assuming the same velocity distributions. All data were measured at the maximum of the angular distributions (see following paragraph). Translational energy distributions showed that the energy of surface-scattered product ions was substantially smaller (by about 50–70%) than their incident energy. Peaks of distributions for collisions with the heated tungsten surface were located at somewhat higher energies than for room temperature surfaces. In general, the characteristics of collisions with tungsten and carbon (HOPG) surfaces were similar. This may be attributed to considerable amounts of tungsten carbides on the heated tungsten surfaces, as indicated by the ex situ ESCA analysis (see Section 2.2); incident ions may collide with carbon from the tungsten carbides formed by cracking the surface hydrocarbons upon heating the samples.

Fig. 3 shows a comparison of peak locations for product ion translational energy distributions scattered from tungsten and carbon (HOPG) surfaces (data from Refs. [20,22,24]). The peak values of $P(E'_{tr})$, plotted as a ratio of the peak translational energy of scattered ions, E'^{P}_{tr}, to the incident energy E_{inc}, E'^{P}_{tr}/E_{inc}, are shown as a function of E_{inc}. The fraction of incident energy transferred into product ion translational energy increased somewhat with incident energy. For surfaces heated to 600 °C, the ratio E'^{P}_{tr}/E_{inc} was usually 5–30% higher than for room temperature surfaces. Data for tungsten and carbon (HOPG) were in most cases very similar.

For $C_2D_4^{\bullet+}$ collisions, translational energy distributions were measured for incident angles of 60° (Figs. 2 and 3) and 45°. For the incident angle of 45°, $P(E'_{tr})$ peaked at 17% (21%), 21% (22%), and 19% (48%) (numbers in parentheses referring to measurements on heated surface) for incident energies of 15.4 eV, 30.9 eV, and 45.4 eV, respectively. The values can be compared with those for an incident angle of 60°, namely 21% (23%), 25% (36%), and 48% (53%) (see data in Figs. 2 and 3). The fraction of incident energy in product translational energy thus increased with decreasing incident angle (measured with respect to the surface normal), in agreement with our earlier observations [25].

3.4. Angular distributions of product ions

Fig. 4 shows examples of angular distributions of product ions scattered from room temperature and heated tungsten surfaces at the collision energy of 30.9 eV (incident angle 60°). In general, the angular distributions were very similar to those obtained with carbon (HOPG) surfaces [20,22]. The angular distributions peaked at sub-specular angles of 70–75° and there was only a very small shift of the angular maximum to higher scattering angles with increasing incident energy (from 70–75° to 75–80° for energies from 15 eV to 45 eV). Analogous behavior was found in studies of CD_5^+ on HOPG surfaces [20]. Peaking of the angular distributions at sub-specular angles was presumably caused by the inelastic character of surface collisions [25,26]. Angular data were important in estimation of survival probabilities, S_a (see Section 3.1).

4. Conclusions

(1) The ion survival probability of the investigated ions for both room temperature and heated W surfaces was in general 2–15 times smaller than on carbon (HOPG) surfaces. Ion survival probability tended to be smaller for radical cations ($CD_4^{\bullet+}$ and $C_2D_4^{\bullet+}$) than for closed-shell ions (CD_5^+ and $C_2H_5^+$). For the incident angle of 60° (to the surface normal) the values of S_a(W) were 0.03% for $CD_4^{\bullet+}$, 0.2% for $C_2D_4^{\bullet+}$, 0.5–4% for CD_5^+, and 0.2–2% for $C_2H_5^+$.

(2) Product ion mass spectra from collisions of radical cations $CD_4^{\bullet+}$ and $C_2D_4^{\bullet+}$ on room temperature W surfaces, suggested the occurrence of simple projectile ion fragmentation and of reactions with hydrocarbons adsorbed on to the room temperature surface. These observations are similar to those for collisions with room temperature carbon (HOPG) surfaces. Reactions with absorbed hydrocarbons were namely H-atom transfer leading to the formation of CD_4H^+($C_2D_4H^+$) and their fragmentation products, and carbon-chain build-up reactions (formation of $C_2X_3^+$ and $C_3X_3^+$, X = H, D in reactions with terminal CH_3– groups of the surface hydrocarbons). Closed-shell ions (CD_5^+ and $C_2H_5^+$) exhibited only fragmentation processes. On heated surfaces, only fragmentation of the incident projectile ions was observed.

(3) Translational energy and angular distributions of product ions from collisions with W surfaces were very similar to data obtained earlier for carbon (HOPG) surfaces. Translational energy distributions (at the maximum of the angular distribution) peaked at 30–50% of incident energy; the peak shifted somewhat to higher energies with increasing incident energy. In collisions with W surfaces heated to 600 °C the maximum of the translational energy distributions was 5–30% higher than with room temperature W surfaces.

(4) The similarity of results on heated tungsten and HOPG surfaces may be caused by substantial coverage of W surfaces by tungsten carbide, originating from cracked surface hydrocarbons.

Acknowledgments

This paper is dedicated to Eugen Illenberger in appreciation of his contributions to ion chemistry. The authors thank Zdeněk Bastl for carrying out the ESCA analysis of the W samples used. Partial support of this research by grants from the Grant Agency of the Academy of Sciences of the Czech Republic (Nos. 4040405 and IAA 400400702), and by the Association EURATOM-IPP.CR in cooperation with Association EURATOM ÖAW, is gratefully acknowledged. The content of the publication is the sole responsibility of its publishers and it does not necessarily represent the views of the EU Commission or its services.

References

[1] J.W. Rabalais (Ed.), Low Energy Ion-surface Interactions, John Wiley, New York, 1994.
[2] R.G. Cooks, T. Ast, M.D.A. Mabud, Int. J. Mass Spectrom. 100 (1990) 209.
[3] L. Hanley (Ed.), Polyatomic Ion-surface Interactions, Int. J. Mass Spectrom. 174 (1994) 1.
[4] V. Grill, J. Shen, C. Evans, R.G. Cooks, Rev. Sci. Instrum. 72 (2001) 3149.
[5] W.O. Hofer, J. Roth (Eds.), Physical Processes of the Interaction of Fusion Plasmas with Solids, Academic Press, San Diego, CA, 1996.
[6] Z. Herman, J. Am. Soc. Mass Spectrom. 14 (2003) 1360.
[7] V.H. Wysocki, J.L. Jones, J.M. Ding, J. Am. Chem. Soc. 113 (1991) 8969.
[8] B.E. Winger, R.K. Julian, R.G. Cooks, C.E.D. Chidsey, J. Am. Chem. Soc. 113 (1991) 8967.
[9] J. Laskin, E. Denisov, J.H. Futrell, J. Phys. Chem. B 105 (2001) 1895.
[10] R.G. Cooks, J.W. Amy, M.E. Bier, J.C. Schwarz, K.L. Schey, Adv. Mass Spectrom. 11 (1989) 33.
[11] A.L. McCormack, J.L. Jones, V.H. Wysocki, J. Am. Soc. Mass Spectrom. 3 (1992) 859.
[12] A.L. McCormack, A. Somogyi, A.R. Dongre, V.H. Wysocki, Anal. Chem. 65 (1993) 2859.
[13] S. Rakov, E. Denisov, J. Laskin, J.H. Futrell, J. Phys. Chem. A 106 (2002) 2781.
[14] J. Alvarez, J.H. Futrell, J. Laskin, J. Phys. Chem. A 110 (2006) 1678.
[15] C.M. Jones, R.L. Beardsley, A.S. Gelhena, S. Dagan, G. Cheng, V.H. Wysocki, J. Am. Chem. Soc. 128 (2006) 15044.
[16] J. Laskin, J.H. Futrell, J. Chem. Phys. 119 (2003) 3413.
[17] O. Meroueh, W.L. Hase, J. Am. Chem. Soc. 124 (2002) 1524.
[18] E. Martinez-Nunez, A. Rahaman, W.L. Hase, J. Phys. Chem. C 111 (2007) 354.
[19] V. Philipps, J. Roth, A. Loarte, Conclusions of the Conference of the Task Force "Plasma–Wall Interactions", Cadarache, CEA, October 17–19, 2005.
[20] J. Roithová, J. Žabka, Z. Dolejšek, Z. Herman, J. Phys. Chem. B 106 (2002) 8293.
[21] J. Žabka, Z. Dolejšek, J. Roithová, V. Grill, T.D. Märk, Z. Herman, Int. J. Mass Spectrom. 213 (2002) 145.
[22] J. Jašík, J. Žabka, L. Feketeová, I. Ipolyi, T.D. Märk, Z. Herman, J. Phys. Chem. A 109 (2005) 10208.
[23] J. Jašík, J. Roithová, J. Žabka, A. Pysanenko, L. Feketeová, I. Ipolyi, T.D. Märk, Z. Herman, Int. J. Mass Spectrom. 249–250 (2006) 162.
[24] A. Pysanenko, J. Žabka, F. Zappa, T.D. Märk, Z. Herman, Int. J. Mass Spectrom. 273 (2008) 35.
[25] J. Kubišta, Z. Dolejšek, Z. Herman, Eur. Mass Spectrom. 4 (1998) 311.
[26] J. Žabka, Z. Dolejšek, Z. Herman, J. Phys. Chem. A 106 (2002) 10861.